

Adaptive optics by incoherent digital holography

Myung K. Kim

Department of Physics, University of South Florida, Tampa, Florida 33620, USA
(mkkim@usf.edu)

Received April 5, 2012; revised May 21, 2012; accepted May 22, 2012;
posted May 23, 2012 (Doc. ID 166149); published June 26, 2012

Adaptive optics in astronomical and other imaging systems allows compensation of aberrations introduced by random variations of the refractive index in the imaging path. I propose what I believe is a new type of adaptive optics system that dispenses with the hardware lenslet arrays and deformable mirrors of conventional systems. Theoretical and experimental studies show that wavefront sensing and compensation can be achieved by numerical processing of digital holograms of the incoherent object and a guide star. The incoherent digital holographic adaptive optics is seen to be particularly robust and efficient, with envisioned applications in astronomical imaging, as well as fluorescence microscopy and remote sensing. © 2012 Optical Society of America

OCIS codes: 110.1080, 090.1995, 350.1260.

The concept of adaptive optics (AO), put forward at least several decades ago, is based on sensing the wavefront and adjusting the optical system to compensate for any distortion [1,2]. The development of wavefront sensors and compensators with sufficient level of performance was crucial to implementation of the AO in large telescope systems that began in the 1990s. Remarkable astronomical images have been obtained using ground-based telescopes with AO compensation of atmospheric turbulence, whose image quality can even surpass space-based telescopes under favorable conditions. A common method of wavefront sensing is the Shack–Hartmann sensor consisting of a lenslet array and a CCD camera underneath it, in addition to another separate camera for actual imaging. For wavefront compensation, deformable mirrors or other spatial light modulators (SLMs) are used.

The number of sensor subapertures limits the spatial bandwidth of measurable aberration, while the number and types of actuators in the modulator limit the accuracy and bandwidth of corrections [3]. Accurate registration of the sensor and modulator is also an issue, as well as the speed and accuracy of computation and optomechanical feedback. Specifications of wavefront sensors and modulators are governed by the key parameters of atmospheric turbulence including the Fried parameter, the isoplanatic angle and the Greenwood frequency [4].

An AO system for holographic coherent imaging was recently introduced [5]. It replaces the wavefront sensor and corrector hardware components with numerical processing by digital holography for wavefront measurement and compensation [6,7]. The principle of aberration compensation is a well-known characteristic of holography [8]. Compensation of low-order aberrations has been demonstrated in digital holographic microscopy (DHM) [9], and the concept of numerical parametric lens has been introduced that can shift, magnify, and compensate for aberrations [10]. On the other hand, a majority of common imaging systems require working with incoherent sources, such as astronomy, fluorescence microscopy, and photography. A number of techniques, including achromatic fringes and conoscopic systems, have been put forward for holography of incoherent sources since early years of conventional holography [11,12]. Adaptation of digital holography to these concepts

has been fruitful, though not fully exploited [13,14]. Scanning holography takes a unique approach to incoherent holography but requires mechanical scanning [15]. Recently, Rosen *et al.* introduced the Fresnel incoherent correlation holography (FINCH), where formation of Fresnel interference of incoherent point sources is combined with phase-shifting digital holography (PSDH) to extract complex amplitude of optical fields from arbitrary incoherent objects [16,17]. This approach is a powerful technique that removes many barriers for practical development of holography using incoherent light.

In this Letter, I introduce what I believe is a new method of AO to measure and compensate aberrations based on incoherent digital holography with a modified FINCH interferometer. The method—incoherent digital holographic adaptive optics (IDHAO)—is particularly robust and efficient, as I demonstrate with theoretical, simulation, and experimental studies. Figure 1 illustrates a self-referenced interferometer used in the experiment. It is a modification of the FINCH interferometer, where the pixel-sharing SLM is replaced with a modified Michelson interferometer. The object field consists of a set of incoherent point sources (e.g., LEDs). The collimated light from each point source illuminates the interferometer. The beam splitter (BS) generates two copies of the input field. One is reflected to a plane mirror M1 and the other transmitted to a long-focus concave mirror M2. The two parts arrive at the CCD camera with different curvatures. Because a light field is always coherent with respect to a

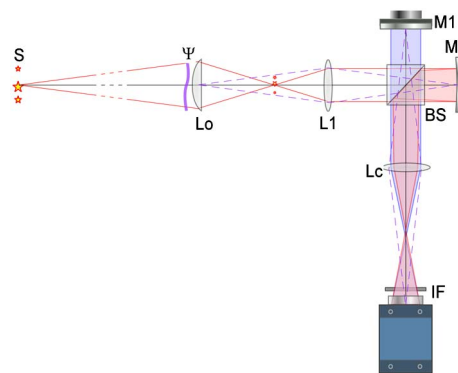


Fig. 1. (Color online) Optical schematic of IDHAO system: S, object plane, including a guide star; L, lenses; M1, piezo-mounted plane mirror; M2, curved mirror; Ψ , aberrator; IF, interference filter.

copy of it, they interfere and form Fresnel zone-like fringes. The piezo-mounted mirror M1 is used for a phase-shifting procedure [18] to extract the phase and the complex field at the CCD plane, which can be expressed as, assuming unit magnification,

$$\begin{aligned} H(x_h, y_h) &= \iint dx_o dy_o I_o(x_o, y_o) Q_{Z_i}(x_h - x_o, y_h - y_o) \\ &= [I_o \odot Q_{Z_i}](x_h, y_h), \end{aligned} \quad (1)$$

where $I_o(x_o, y_o)$ represents the object intensity pattern, $Q_{Z_i}(x - x_o, y - y_o)$ is the quadratic phase factor of a spherical wave centered at (x_o, y_o, Z_i) , and the symbol \odot stands for convolution. On the other hand, if we model the phase aberration with a phase function $\Psi(x_1, y_1)$ present at the lens plane Lo, and if that plane is imaged by the lens L1 onto the mirrors M1 and M2, then the corresponding complex hologram becomes

$$H_\Psi(x_h, y_h) = [I_o \odot G_\Psi](x_h, y_h), \quad (2)$$

where $G_\Psi(x, y)$ is the hologram of a guide star, acquired separately using a point source at the center of the object plane. The object intensity I_o can be recovered by subtracting the phase of G_Ψ from H_Ψ in the Fourier domain, as long as the autocorrelation of G_Ψ is a delta function.

An example from a simulation study is shown in Fig. 2. The assumed phase aberration [Fig. 2(b)] leads to vortex-like structure in the guide star hologram [Fig. 2(e)], as well as in the full-field hologram [Fig. 2(c)]. This prevents

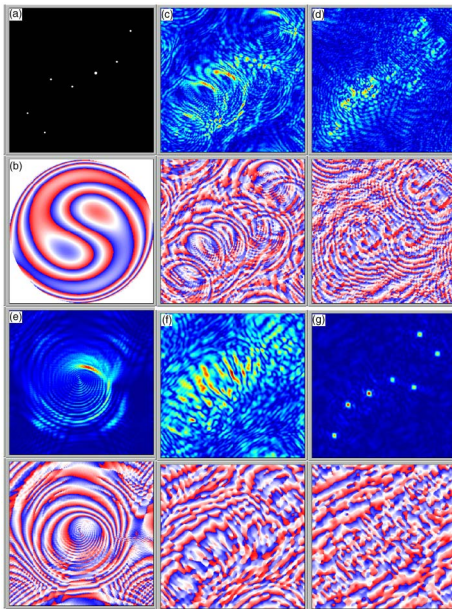


Fig. 2. (Color online) Simulation example of IDHAO: (a) assumed object pattern, (b) assumed phase aberration consisting of Zernike terms $(-0.5)2\pi \times [Z_3^{+1} + Z_5^{-1}]$, (c) amplitude (upper) and phase (lower) of complex hologram, uncorrected, (d) best focus image reconstructed from the uncorrected hologram, (e) hologram of a guide star, (f) corrected hologram by IDHAO, and (g) best focus image reconstructed from the corrected hologram. In all phase profiles, the blue–white–red color map corresponds to the phase range of $[-\pi, \pi]$.

formation of good focus in the reconstructed image [Fig. 2(d)]. On the other hand, the vortex-like structure is replaced with Fresnel lens-like concentric structures in the IDHAO-corrected hologram [Fig. 2(f)] that leads to well-defined focus image [Fig. 2(g)]. Other simulation examples (not presented here) for varying strengths and types of aberration show that the IDHAO process removes the distortions even for fairly serious aberrations.

The apparatus of Fig. 1 was set up using lenses of focal length 100 mm and a concave mirror of focal length 600 mm. The object plane was approximately 700 mm from the objective lens Lo, and its image was near the front focus of L1. Another lens, Lc, in front of the camera is adjusted so that the two spherical wave components from a guide star arrive at the camera with the same illumination area but different curvatures, a condition that optimizes the fringe contrast and resolution [19]. For the aberrator, a clear plastic piece with an irregular surface or astigmatic eyeglass lens was used. A 600 nm interference filter was used to narrow the line width to about 10 nm for halogen-lamp illumination. The piezo-transducer for mirror M1 is driven with a sawtooth output of a digital function generator and four phase-shift holograms are acquired at 20 fps. Hologram acquisition, reconstruction, and aberration compensation are carried out by LabVIEW-based programs. The entire cycle takes only a few seconds, including file write/read and without any attempt to optimize the speed.

The principles of IDHAO were verified in experiments using three LEDs (Fig. 3). First, four frames of holograms were captured by the camera, one of them shown in [Fig. 3(e)], which are combined to extract the complex hologram [Fig. 3(a)]. Numerical propagation from the hologram to an appropriate distance yields the image [Fig. 3(b)]. Placing the aberrator—a piece of plastic with an irregular surface—near Lo severely distorts the holograms [Figs. 3(f)–3(c)], and the best focus image [Fig. 3

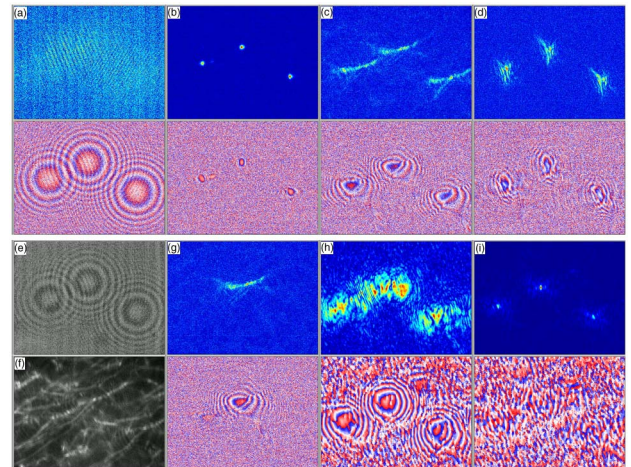


Fig. 3. (Color online) Experimental demonstration of IDHAO using three red LEDs as the object: (a) complex hologram without aberrator, (b) reconstructed image, (c) complex hologram with aberrator, (d) best focus image reconstructed from the uncorrected hologram, (e) one of four holograms captured by camera without aberrator, (f) one of four holograms with the aberrator, (g) complex hologram of one LED as guide star, (h) corrected hologram by IDHAO, and (i) best focus image reconstructed from the corrected hologram.

(d) is seriously degraded. A guide star hologram [Fig. 3(g)], acquired by leaving only one of the LEDs on, is used to compensate the aberration, resulting in the corrected hologram [Fig. 3(h)]. Notice that the phase profile of [Fig. 3(h)] has better Fresnel lens-like concentric structures compared to [Fig. 3(c)], leading to reconstructed image [Fig. 3(i)], with comparable quality to the unaberrated image [Fig. 3(b)]. Note that a direct image, when the camera is moved to an image plane while one of the mirrors is covered, was seen to be qualitatively similar to the uncorrected holographic image [Fig. 3(d)].

Another example of IDHAO is shown in Fig. 4, where the object is a resolution target illuminated with a halogen lamp through a piece of frosted glass, while the guide star is provided by an LED placed close in front of the resolution target. First, the IDHAO is carried out without an aberrator. The reconstructed image [Fig. 4(a)] from the uncorrected hologram was clear enough, though it required some adjustment of contrast for presentation. There is no aberrator and therefore no aberrations to correct, but application of the IDHAO process results in some loss of resolution but improvement in noise and contrast in the final image [Fig. 4(b)]. When an aberrator—an astigmatic eyeglass lens—is introduced, the difference between the uncorrected [Fig. 4(c)] and corrected [Fig. 4(d)] images is more pronounced. The process simultaneously removes distortion, displacement due to tilt, and noise. The fringe contrast in the raw holograms was quite low and the extracted complex hologram had significant noise in the form of a background haze. The IDHAO process substantially suppressed such noise in the final image [Fig. 4(d)]. The effect of noise reduction by IDHAO is most evident in Figs. 4(e) and 4(f), where a chess pawn is imaged with a high-brightness red LED illumination. A separate LED is used as a guide star and no aberrator was in place. Again, the application of the IDHAO process significantly improved the final image quality.

I have introduced what I believe is a new method of AO using incoherent digital holography. Both the simulation and experimental results show that the compensation of the aberration is robust and efficient, clearly capable of repairing even highly distorted images. It not only compensates optical aberrations represented by Zernike polynomial terms, but also suppresses noise due to a weak signal. This effect is tentatively attributed to the filtering by delta-function-like autocorrelation of the guide star hologram. The new IDHAO system, substantially reduces the complexity, and very likely the cost, of the optomechanical system compared to any existing AO systems. The wavefront sensing and correction of IDHAO have almost the full resolution of the CCD camera. This approach does not involve electronic–numerical–

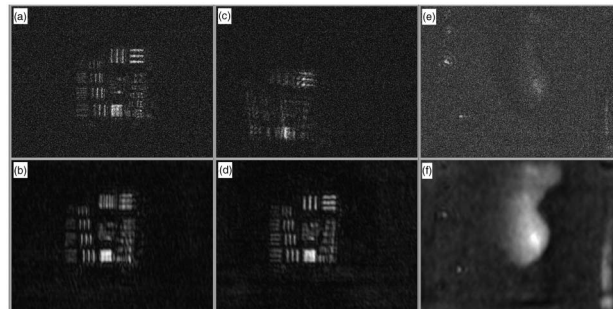


Fig. 4. Experimental demonstration of IDHAO of extended objects. Upper row, reconstructed images from uncorrected hologram; lower row, from corrected hologram. Left, resolution target without aberrator; middle, resolution target with an aberrator; right, chess pawn, no aberrator but low fringe contrast.

mechanical feedback, the numerical computation of the holographic images is faster than the conventional AO feedback loop, and the dynamic range of the deformation measurement is essentially unlimited. I envision applications of IDHAO in astronomical telescopes, as well as a wide range of other application areas that have been precluded in conventional holography, such as fluorescence microscopy and remote sensing. Additional theoretical and experimental details will be published elsewhere.

References

1. R. K. Tyson, *Principles of Adaptive Optics* (CRC Press, 2011).
2. J. M. Beckers, *Annu. Rev. Astron. Astrophys.* **31**, 13 (1993).
3. M. C. Liu, <http://arxiv.org/abs/astro-ph/0609207> (2006).
4. R. K. Tyson, *Introduction to Adaptive Optics* (SPIE, 2000).
5. C. G. Liu and M. K. Kim, *Opt. Lett.* **36**, 2710 (2011).
6. M. K. Kim, *SPIE Rev.* **1**, 018005 (2010).
7. M. K. Kim, *Digital Holographic Microscopy: Principles, Techniques, and Applications* (Springer, 2011).
8. J. Upatnieks, A. V. Lugt, and E. N. Leith, *Appl. Opt.* **5**, 589 (1966).
9. L. Miccio, D. Alfieri, S. Grilli, P. Ferraro, A. Finizio, L. De Petrocellis, and S. D. Nicola, *Appl. Phys. Lett.* **90**, 041104 (2007).
10. T. Colomb, F. Montfort, J. Kuhn, N. Aspert, E. Cuche, A. Marian, F. Charriere, S. Bourquin, P. Marquet, and C. Depeursinge, *J. Opt. Soc. Am. A* **23**, 3177 (2006).
11. E. N. Leith and J. Upatnieks, *J. Opt. Soc. Am.* **57**, 975 (1967).
12. G. Sirat and D. Psaltis, *Opt. Lett.* **10**, 4 (1985).
13. S. G. Kim, B. Lee, and E. S. Kim, *Appl. Opt.* **36**, 4784 (1997).
14. L. M. Mugnier, G. Y. Sirat, and D. Charlot, *Opt. Lett.* **18**, 66 (1993).
15. T. C. Poon, *J. Opt. Soc. Korea* **13**, 406 (2009).
16. J. Rosen and G. Brooker, *Opt. Lett.* **32**, 912 (2007).
17. J. Rosen and G. Brooker, *Nat. Photon.* **2**, 190 (2008).
18. I. Yamaguchi and T. Zhang, *Opt. Lett.* **22**, 1268 (1997).
19. G. Brooker, N. Siegel, V. Wang, and J. Rosen, *Opt. Express* **19**, 5047 (2011).